

Single-Molecule Studies Reveal Dynamics of DNA Unwinding by the Ring-Shaped T7 Helicase

Daniel S. Johnson,¹ Lu Bai,¹ Benjamin Y. Smith,¹ Smita S. Patel,² and Michelle D. Wang^{1,*}

¹Department of Physics, Laboratory of Atomic and Solid State Physics, Cornell University, Ithaca, NY 14853, USA

²Department of Biochemistry, UMDNJ-Robert Wood Johnson Medical School, 675 Hoes Lane, Piscataway, NJ 08854, USA

*Correspondence: mdw17@cornell.edu

DOI 10.1016/j.cell.2007.04.038

SUMMARY

Helicases are molecular motors that separate DNA strands for efficient replication of genomes. We probed the kinetics of individual ring-shaped T7 helicase molecules as they unwound double-stranded DNA (dsDNA) or translocated on single-stranded DNA (ssDNA). A distinctive DNA sequence dependence was observed in the unwinding rate that correlated with the local DNA unzipping energy landscape. The unwinding rate increased ~ 10 -fold (approaching the ssDNA translocation rate) when a destabilizing force on the DNA fork junction was increased from 5 to 11 pN. These observations reveal a fundamental difference between the mechanisms of ring-shaped and nonring-shaped helicases. The observed force-velocity and sequence dependence are not consistent with a simple passive unwinding model. However, an active unwinding model fully supports the data even though the helicase on its own does not unwind at its optimal rate. This work offers insights into possible ways helicase activity is enhanced by associated proteins.

INTRODUCTION

Helicases are vital enzymes that separate a double-stranded nucleic acid (dsNA) into two single-stranded nucleic acids (ssNA) during DNA replication, DNA repair, DNA recombination, and transcription termination (Lohman and Bjornson, 1996; Patel and Picha, 2000). They are processive molecular motors which utilize chemical energy from NTP hydrolysis to translocate along ssNA. As they encounter a ss/dsNA fork junction, they are capable of moving the junction forward, thereby catalyzing the unwinding of the dsNA. Many important functions and properties of these enzymes have been brought to light in the past few decades through a combination of structural, biochemical, and, more recently, single-molecule

studies (e.g., Kim et al., 1998; Singleton et al., 2000; Ene-mark and Joshua-Tor, 2006; Dillingham et al., 2000; Maluf et al., 2003; Kaplan and O'Donnell, 2004; Brendza et al., 2005; Dohoney and Gelles, 2001; Spies et al., 2003; Perkins et al., 2004; Dessinges et al., 2004; Myong et al., 2005; Dumont et al., 2006; Lee et al., 2006). However, one intriguing question which has been under much investigation but still remains unanswered is how a helicase couples its translocation along a ssNA to the unwinding of a dsNA.

Two competing mechanisms have been put forth that differ in the thermodynamic and kinetic natures of the interactions of a helicase with a fork junction (Lohman and Bjornson, 1996; von Hippel and Delagoutte, 2001; Soutanas and Wigley, 2001; Betterton and Jülicher, 2003). The simplest scenario is the “passive” unwinding mechanism. Here the dsNA at the junction is transiently opened solely by thermal fluctuations, and the helicase may forward translocate onto the newly available ssNA, thereby preventing it from reannealing. Thus the helicase unwinds the dsNA by simply trapping the thermally frayed ssNA at the junction. In the alternative “active” unwinding mechanism, as the helicase encounters a junction, it actively destabilizes the dsNA near the junction and therefore shifts the equilibrium of the fork toward opening. The degree of the helicase's active involvement in the unwinding mechanism depends on the extent to which the helicase shifts the equilibrium of junction opening, which in turn depends on the helicase's NTPase mechanism and the nature of its interaction with the fork.

The passive unwinding mechanism is appealing due to its simplicity. Early calculations indicated that the replication fork might unwind via a passive mechanism. It was proposed that the trapping of the thermally fluctuating fork alone might be sufficient to account for the rapid rate of replication (Chen et al., 1992; Delagoutte and von Hippel, 2002). Similarly, it has been proposed that Rho helicase, a ring-shaped transcription termination factor, might effectively be passive, its unwinding of the RNA/DNA hybrid driven solely by thermally induced fraying of the hybrid junction (Geiselmann et al., 1993; von Hippel and Delagoutte, 2001). Structural studies of a nonring-shaped helicase, hepatitis C virus NS3, have indicated

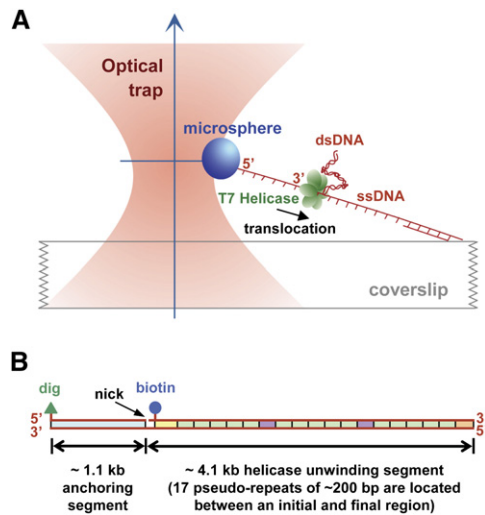


Figure 1. Experimental Configuration

(A) This cartoon illustrates the experimental configuration for the observation of the unwinding of dsDNA by a single T7 helicase (not to scale). One strand of the dsDNA to be unwound was attached to a trapped microsphere via a biotin/streptavidin connection. The other strand was anchored to a microscope coverslip surface via a dig/antidig connection on a dsDNA anchoring segment. The microsphere was held in a feedback-enhanced optical trap so that its position relative to the trap center and the force on it could be measured. Helicase unwinding of dsDNA was monitored as an increase in the ssDNA length. Helicase did not unwind the dsDNA anchoring segment because it prefers two ssDNA regions at a fork junction (Ahnert and Patel, 1997).

(B) The DNA construct contained both digoxigenin (dig) and biotin labels for binding to the coverglass and microsphere, respectively. The dig label was located at one end of the DNA construct and was bound to an antidigoxigenin-coated coverglass. The biotin label was on one strand of the DNA and was bound to a streptavidin-coated microsphere. On the same strand near this biotin label was a nick in the ssDNA. The nick allowed the DNA to be mechanically unwound (unzipped) when the DNA anchor on the coverslip was moved away from the microsphere.

a passive mechanism for unwinding (Kim et al., 1998). However, biochemical and/or structural studies of Rep, PcrA, and UvrD, all of which are nonring-shaped helicases, favor an active mechanism for unwinding (Wong and Lohman, 1992; Amaratunga and Lohman, 1993; Soutanas et al., 2000; Fischer et al., 2004). While the detailed nature of the mechanism (“active rolling” versus “inchworm”) and the stoichiometry (dimer versus monomer) of the enzymes may still be under debate, a consensus seems to have emerged that these helicases interact with the dsDNA ahead of the junction and thus are thought to destabilize the fork to facilitate unwinding. Taken together, there is evidence that some nonring-shaped helicases may use a passive unwinding mechanism while others may use an active mechanism. However, much less is known about the unwinding mechanism of ring-shaped helicases.

T7 helicase is a model enzyme for understanding hexameric ring-shaped helicases (Richardson, 1983; Patel and Hingorani, 1993) and perhaps helicases in general.

As a critical part of the relatively simple T7 bacteriophage replication complex, T7 helicase consists of homologous monomers that form a ring-shaped hexamer in the presence of dTTPs and ssDNA (Patel and Hingorani, 1993; Egelman et al., 1995). It is known to bind one strand of dsDNA within its central channel (Egelman et al., 1995) while excluding the complementary strand (Hacker and Johnson, 1997; Ahnert and Patel, 1997). During translocation from 5' to 3' on ssDNA (Tabor and Richardson, 1981), the helicase unwinds dsDNA as it hydrolyzes dTTP (Matson and Richardson, 1983; Matson et al., 1983).

In this report we present single-molecule mechanical measurements in conjunction with a detailed thermodynamic and kinetic analysis to distinguish between a passive and active unwinding mechanism. First, the rate of helicase translocation along ssDNA was directly measured using a novel single-molecule assay. Since helicase did not have to work against a fork junction, this established the maximum rate for helicase translocation. Second, the rate of helicase unwinding dsDNA was directly measured. The unwinding rate increased dramatically with a force destabilizing the fork and at high force approached the ssDNA translocation rate. Further, the unwinding rate showed distinctive sequence dependence: fast at AT-rich regions and slow at GC-rich regions. Third, in order to quantitatively correlate unwinding rate with the physical barrier that the helicase encountered during unwinding, the dsDNA was mechanically unzipped to determine the sequence-dependent unzipping force. Fourth, sequence-dependent kinetic models for both passive and active mechanisms were formulated to explain the helicase unwinding rate. Our data is not accounted for by the simple passive unwinding model but instead supports an active unwinding model in which the helicase partially destabilizes the fork junction to facilitate unwinding.

RESULTS

Single-Molecule Helicase Assay

Both the measurements for ssDNA translocation and unwinding began with a similar experimental configuration (Figure 1; Johnson et al., 2004; Experimental Procedures) based on a DNA-unzipping technique we previously developed (Koch et al., 2002). An unwinding segment consisting of 17 pseudorepeats each of ~200 base pair (bp) was ligated to an anchoring DNA segment (Figures 1B and S1) and suspended between an optically trapped microsphere and the glass coverslip surface (Figure 1A). The anchoring and the unwinding segments of the DNA template were joined by a single strand only; the nick in the opposite strand allowed the two DNA strands to separate when the coverslip was moved away from the optical trap. Initially ~400 bp of dsDNA were mechanically unwound (unzipped) to generate a ssDNA region by movement of the coverslip relative to the trapped microsphere (Figure 2, step 1). Freely diffusing helicase could load onto the ssDNA (Tabor and Richardson, 1981; Ahnert and Patel, 1997), translocate from 5' to 3', and subsequently unwind

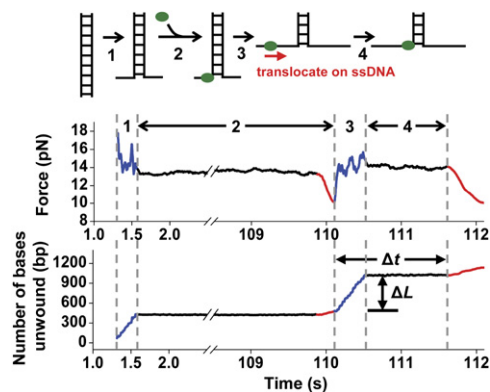


Figure 2. Experimental Method for Measurements of Helicase Translocation along a ssDNA and a Typical Data Set

The experimental procedures were: (1) mechanically unwind ~ 400 bp of dsDNA at a constant velocity of 1400 bp/s to produce a ssDNA loading region, (2) maintain the DNA extension until force drops below a threshold indicating helicase unwinding of the DNA fork, (3) mechanically unwind another ~ 500 bp (ΔL) of dsDNA to generate ssDNA for helicase translocation, and (4) maintain new DNA fork position until force drops again indicating the helicase has caught up with the fork. The blue regions represent the two mechanical unwinding steps, and the red regions represent the two helicase unwinding events with intervening time Δt . Helicase translocation velocity on ssDNA was computed as $\Delta L/\Delta t$.

the remaining dsDNA. This 400 nucleotide (nt) length of ssDNA was maintained under ~ 14 pN tension until a helicase began to unwind the dsDNA, resulting in an increase of ssDNA length and thereby a decrease in its tension (Figure 2, step 2). The helicase binding time was dependent on the length of ssDNA initially unzipped as well as the helicase concentration (data not shown). To ensure that we were measuring the kinetics of a single T7 helicase, we used a low helicase monomer concentration (2.0 nM) so that the average helicase arrival time at the fork junction (~ 80 s; Figure 3A, Supplemental Discussion) was significantly longer than the typical ssDNA translocation and dsDNA unwinding times.

This configuration provided several advantages for detecting motions of individual helicase molecules. First, a helicase did not need to be bound to any surfaces for its motion to be monitored. Thus, the helicase did not need to be tagged for single-molecule measurements, and the helicase itself was not under direct mechanical stress. Second, since a helicase was not able to bind or unwind until a ssDNA loading region was generated mechanically, the start of each measurement could be independently initiated for each microsphere-tethered DNA molecule. This allowed for efficient use of the sample. Third, for each bp of the dsDNA unwound, 2 nt of ssDNA were released, providing an amplification of the detection of the helicase motion.

Fast Translocation of the Helicase on ssDNA

The first experiment used a novel method to investigate the ssDNA translocation rate of helicase on long stretches

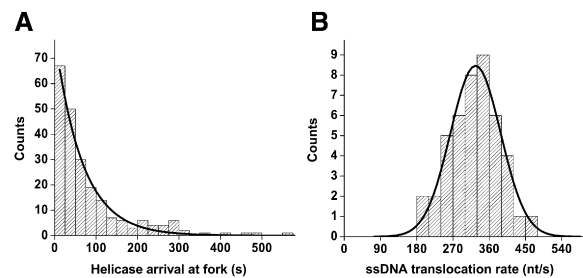


Figure 3. Measurements of Helicase Arrival Time at the Fork Junction and Helicase Translocation Velocity on ssDNA

(A) Measurement of the time it took a helicase to bind to the 400 bp ssDNA loading region and then reach the DNA junction. With the helicase concentration used in our experiments (2 nM monomer), this time followed a single exponential distribution (fit in red) with an average time of ~ 80 s ($N = 237$). This average helicase arrival time at the junction was much longer than the typical observation time for subsequent ssDNA translocation or DNA unwinding measurements (see Supplemental Discussion). Therefore, it was unlikely that more than one helicase acted on the same DNA template.

(B) A histogram of ssDNA helicase translocation rate. Data were pooled from many measurements, and the pooled histogram was well fit by a Gaussian distribution with a mean of 322 nt/s and a standard deviation of 62 nt/s.

of ssDNA. Once a T7 helicase was detected at the fork junction, as determined by a tension drop below a threshold value (~ 10 pN), the coverslip was quickly moved to mechanically unwind another ~ 500 bp (ΔL) of downstream dsDNA, thereby providing a segment of ssDNA for helicase translocation. After a time Δt , the helicase caught up with the new junction position, resulting in another tension drop (Figure 2, steps 3 and 4). The helicase ssDNA translocation rate was then obtained from $\Delta L/\Delta t$. The ssDNA translocation rate of different helicase molecules has a Gaussian distribution with a mean translocation rate of 322 ± 62 nt/s (mean \pm sd) at $\sim 25^\circ\text{C}$ (Figure 3B; Experimental Procedures). This broad distribution could be a result of pausing kinetics in ssDNA translocation and/or heterogeneity in helicase molecules. (We also measured this rate over a distance of ~ 2800 nt and found it to be essentially identical: 320 ± 44 nt/s.) The average ssDNA translocation rate measured in bulk at 18°C was 130 nt/s (Kim et al., 2002), and the rate at 25°C was estimated to be 2- to 3-fold higher (S.S.P., unpublished data), consistent with our measurements. It should be noted that in our single-molecule assay the translocation rate on ssDNA was measured under ssDNA tension of ~ 14 pN. However, from observations of reverse motion during unwinding (see below) we have evidence that the translocation rate was not dependent on the tension in the ssDNA (Figure S2C).

Helicase Unwinding Rate Is DNA Sequence Dependent

Using similar methods, the kinetics of helicase unwinding of dsDNA were measured under constant tension in ssDNA. After the helicase bound to the ssDNA loading

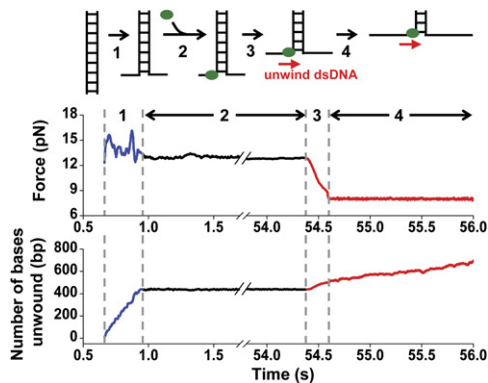


Figure 4. Experimental Method for the Determination of Helicase Unwinding Velocity under a Constant Force and a Typical Data Set

The experimental procedures were: (1) mechanically unwind ~400 bp of dsDNA to produce a ssDNA loading region, (2) maintain the DNA extension until force drops indicating helicase is unwinding dsDNA at the junction, (3) allow force to continue to drop until force reaches a desired value, and (4) maintain constant force while helicase is unwinding dsDNA. The blue (red) region of the data represents the mechanical (helicase) unwinding.

region and began to unwind the dsDNA (Figure 4, steps 1 and 2), feedback control allowed us to follow the fork junction motion in real-time while keeping the tension in the ssDNA constant (Figure 4, steps 3 and 4). This helicase-loading technique allowed for measurements to be conducted at tensions under which the DNA would normally reanneal if the helicase were not present, consistent with the helicase acting as a physical barrier preventing the DNA near the junction from reannealing (von Hippel and Delagoutte, 2001). As the helicase unwound dsDNA, the DNA junction advanced smoothly, with only occasional pauses (Figures 6A and S3). Sometimes the newly generated ssDNA reannealed almost instantaneously, which we attributed to either the helicase dissociating from the DNA or the DNA reannealing behind the helicase (Figure S2B). Occasionally, the junction position moved backward on the DNA with finite velocity (Figures S2A and S2C). This reverse movement could be produced by the helicase switching from one ssDNA strand to the other but still moving in the 5' to 3' direction. Such reverse movement has also been previously reported for UvrD and NS3 (Desingues et al., 2004; Dumont et al., 2006). The observed reverse rates (~310 nt/s) were comparable to the ssDNA translocation rate and faster than the dsDNA unwinding rate, which is expected since the helicase was no longer working against the DNA fork.

The unwinding rate showed a distinctive DNA sequence-dependence. The instantaneous unwinding rate averaged over many traces acquired at a force of 11.2 pN displayed a periodicity of ~200 bp (Figure 5A), consistent with the periodicity of pseudorepeats in the DNA (Experimental Procedures). To correlate the helicase sequence-dependent unwinding rate with the corres-

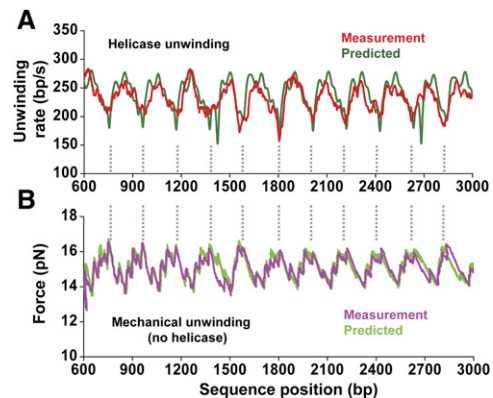


Figure 5. Sequence Dependence of Helicase Unwinding Velocity

(A) Instantaneous velocity of helicase along dsDNA template positions under 11 pN force. The measured curve was obtained by averaging 32 single traces. The measured sequence-dependent velocity agreed well with that predicted from an active model.

(B) Measured and predicted dsDNA mechanical unwinding force on the same DNA sequence. Unzipping force anticorrelates with the helicase unwinding rate in Figure 5A.

ponding DNA base-pairing strength, a separate experiment was conducted in which the DNA was mechanically unwound (unzipped) at a slow velocity in the absence of helicase. In these data, the base-pairing strengths were reflected by the unzipping force (Bockelmann et al., 1997), with low force corresponding to AT-rich regions and high force corresponding to GC-rich regions (Figure 5B). Comparison between Figures 5A and 5B shows that the helicase unwinding rate anticorrelated with the DNA-unzipping force, indicating that it is harder for the helicase to unwind the DNA when the affinity between the two DNA strands is stronger. Additional measurements of unwinding at other forces and on a different DNA sequence again displayed rates which anticorrelated with the unzipping force (Figures S4 and S5), indicating that sequence-dependent unwinding is characteristic of this helicase. The finding that T7 helicase has a sequence-dependent unwinding rate is fully consistent with the force-dependence described below.

Helicase Unwinding Rate Is Strongly Force Dependent

The forces exerted on ssDNA lower the affinity between the two strands and should assist helicase motion. To test this hypothesis, helicase unwinding of dsDNA was measured at various constant forces below the mechanical unzipping force (Figures 6A and S3). The average unwinding rate was found to increase nonlinearly with respect to force, with the rate at low force (29 bp/s at 5.2 pN) approaching that measured in bulk (10–15 bp/s; Jeong et al., 2004; Stano et al., 2005) and the rate at high force (220 bp/s at 11.2 pN) approaching the ssDNA translocation rate (Figure 6B). Previous single-molecule studies of

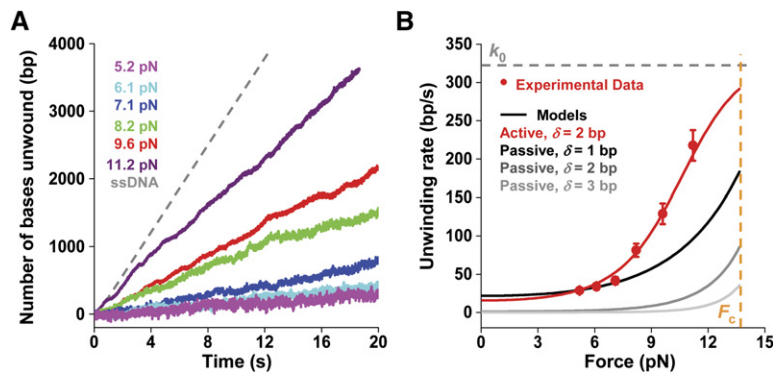


Figure 6. Force-Velocity Measurements during Helicase Unwinding

(A) Example traces of helicase unwinding of dsDNA at various forces. Unwinding velocity varied dramatically with the applied force on ssDNA. (B) Measured force-velocity relation and its comparison with predictions based on various models. Measured force-velocity relation deviated significantly from a simple passive model at step sizes (δ) 1, 2, or 3 bp; larger δ only made the deviation larger. In contrast, an active model with $\delta = 2$ bp and destabilization energy $\Delta G_d = 1.2 k_B T$ per bp over a 6 bp range agrees well with the measurements. Also marked on the plot are the ssDNA translocation rate k_0 and the minimum (critical) DNA mechanical unwinding force F_c for the given sequence. Error bars indicate standard errors of the means.

different helicases found no force-dependence (Dessinges et al., 2004; Dumont et al., 2006). Thus, the unwinding mechanism of this ring-shaped helicase appears to be fundamentally different from the nonring-shaped superfamily 1 and 2 helicases. The increase in unwinding rate with increasing force indicates that the rate of T7 helicase (and perhaps other ring-shaped helicases) is limited by strand separation.

The average length of DNA unwound before reannealing was also dependent on force. At 11.2 pN, most helicase molecules (85%) completely unwound the remaining 3.6 kb DNA, while at 5.2 pN, the average length was only 343 bp (Figure S6). In previous bulk studies, the unwinding processivity of T7 helicase was measured to be ~ 60 bp (Jeong et al., 2004), whereas the processivity on ssDNA has been observed to be 75,000 nt (Kim et al., 2002). These results agree well with our observations that the total unwinding distance increased from low to high force. Interestingly, force-dependent processivity was also found in other helicases (Dessinges et al., 2004; Dumont et al., 2006).

Unwinding Rate Observations Do Not Support a Simple Passive Unwinding Model

The above results for both the ssDNA translocation rate and unwinding rates should allow for the differentiation between passive and active unwinding models for T7 helicase. Since the dsDNA presents a strong physical barrier to the helicase unwinding, qualitative reasoning might suggest that the observed force- and sequence-dependencies imply a passive mechanism of unwinding. Therefore, we first formulated a passive kinetic model in an effort to account for unwinding rates as a function of force (Figure 7B). The basic formulation was similar to the theory of Betterton and Jülicher (2003, 2005) but with an extension to incorporate DNA sequence- and force-dependent fork junction opening kinetics and to allow the helicase step size to be larger than 1 nt.

Consider a case in which the helicase has translocated on the ssDNA (under tension F) in the 5' to 3' direction toward the DNA fork junction and is located at the l^{th} nucleotide from the 5' end (Figure 7A). The helicase translocation rate $k'_0(m)$ may be altered by the presence of the junction, which is open m bases from the helicase with a probability $P(l, m, F)$. Assuming the DNA fork opening/closing events follow rapid equilibrium kinetics, the overall helicase unwinding rate at the l^{th} base is an average over all possible junction positional dependent rates, $k'_0(m)$:

$$k(l, F) = \sum_{m=0}^{\infty} k'_0(m) P(l, m, F). \quad (1)$$

The probability for the DNA to be open m bases from the helicase can be calculated for any given DNA sequence:

$$P(l, m, F) = \frac{\exp[-\Delta G(l+m, F)/k_B T]}{\sum_{m=0}^{\infty} \exp[-\Delta G(l+m, F)/k_B T]}, \quad (2)$$

where $\Delta G(l+m, F)$ is the free energy of the DNA with $n = l+m$ bases opened under tension F relative to its fully duplex form.

In the passive unwinding mechanism, this free energy is composed of two contributions, one from the base-pairing energy of the n opened bases, ΔG_{bp} , and one from the free energy of ssDNA under constant force F , ΔG_{ssDNA} :

$$\begin{aligned} \Delta G_{\text{passive}}(n, F) &= \Delta G_{bp} + \Delta G_{ssDNA} \\ &= \sum_{i=1}^n \Delta G_{bp}(i) - 2n \int_0^F x_{nt}(F') dF', \end{aligned} \quad (3)$$

where $\Delta G_{bp}(i)$ is the free energy change due to loss of the base pairing of the i^{th} base pair along the DNA and $x_{nt}(F)$ is the extension versus force relation for one nucleotide of ssDNA (Figure S7). $\Delta G_{bp}(i)$ and $x_{nt}(F)$ were experimentally determined (Experimental Procedures). Therefore, $\Delta G_{\text{passive}}(n, F)$ was directly computed for a given template location along the DNA sequence at a specified force. In addition, the helicase cannot move forward unless the

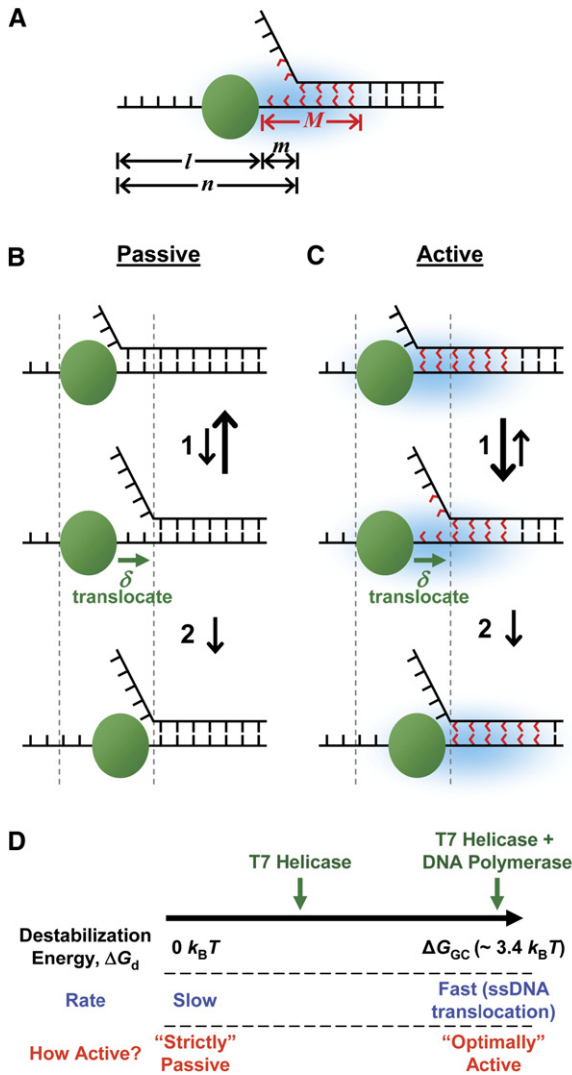


Figure 7. Cartoon of Passive and Active Unwinding Mechanisms

(A) A sketch illustrating the notation used for modeling the helicase movement toward a fork junction. l is the number of nucleotides between the 5' end of the ssDNA and the helicase. m is the number nucleotides of the ssDNA that are open between the helicase and the junction. Therefore, $n = l + m$ is the total number of nucleotides from the end of the ssDNA to the junction. M defines the range of interactions between the helicase and the junction in nt.

(B) Illustration of the passive unwinding mechanism. In this model the DNA fork thermally fluctuates between dsDNA and ssDNA states (step 1). When the amount of ssDNA between the helicase and the junction is greater than or equal to the helicase step size (δ) the helicase may forward translocate (step 2).

(C) Illustration of the active unwinding mechanism. In this model the helicase destabilizes a region (the light blue cloud) of dsDNA near the junction (step 1). This makes the junction more likely to be open so that the helicase is able to step forward (step 2) more frequently.

(D) A cartoon illustrating the degree of activeness in DNA unwinding by helicase. When $\Delta G_d = 0$, the helicase may be considered “strictly” passive, and when $\Delta G_d \sim \Delta G_{GC} (\sim 3.4 k_B T, GC \text{ base-pairing energy})$, “optimally active.” For T7 helicase $\Delta G_d \sim 1 - 2 k_B T$.

available ssDNA in front of it is equal to or greater than its step size (δ). Therefore,

$$k'_{0 \text{ passive}}(m) = \begin{cases} 0, & m < \delta \\ k_0, & m \geq \delta \end{cases} \quad (4)$$

where k_0 represents the helicase ssDNA translocation rate. It is clear from Equation 4 that the larger the step size δ , the slower the helicase will be able to step forward. Equation 1 then allows direct prediction of the unwinding velocity as a function of force and sequence for a given step size.

We compared the predicted unwinding rate versus force relationship to the measurements at different step sizes (Figure 6B). With a step size of 1 bp the model fits the data at low forces, but at higher forces there is a significant deviation between observed and predicted unwinding rates. The model with step sizes greater than 1 bp does not predict the observed velocities at all forces, and the predicted translocation rate is always slower than the observed rate. This result is expected since at larger step sizes the probability for multiple bases to fluctuate open at the DNA fork is very low, and therefore the rate of the helicase is much slower. In general, we concluded that the force-velocity relationship we observed could not be explained by this passive unwinding model. There may exist more complicated passive models that are consistent with our data. However, it is difficult to envision such models without violating the conventional definition of the passive mechanism (Lohman and Bjornson, 1996).

Unwinding Rate Observations Support an Active Unwinding Model

In an alternative active mechanism, the helicase directly destabilizes the dsDNA near the fork junction to facilitate unwinding (Lohman and Bjornson, 1996; von Hippel and Delagoutte, 2001; Betterton and Jülicher, 2003). We formulated an active model that was again based on an extension of the theory of Betterton and Jülicher (2003, 2005; Figure 7C). In this model, when the helicase is far away from the junction, it advances along the ssDNA at its ssDNA translocation rate, just as in the passive model. However, when the helicase is within a characteristic distance of M nucleotides away from the junction, it can interact with the fork. If the interaction potential is repulsive, then the interaction destabilizes a region of the dsDNA near the junction that is within this range M . In this region the helicase can continue to advance forward, albeit at a slower rate. This is as if the helicase encounters a “soft wall” of interaction at the fork. The helicase may advance within this soft-wall until the distance between the helicase and the junction is less than its step size, at which point the helicase encounters a “hard wall.” This soft-wall interaction mediates the active opening of the junction and therefore facilitates the advancement of the helicase.

There are many different ways to formulate the interaction between the helicase and the fork. Consider a simple

scenario where the interaction potential that destabilizes the fork is assumed to decrease linearly with the distance between the helicase and the junction at ΔG_d per nucleotide, within the range of interaction (M ; Betterton and Jülicher 2003, 2005). Therefore, the free energy to open the junction is lowered within this range at a cost of a decrease in the helicase forward translocation rate k_0 active(m):

$$\Delta G_{\text{active}}(l+m, F) = \begin{cases} \Delta G_{\text{passive}}(l+m, F) - m\Delta G_d, & 0 \leq m \leq M \\ \Delta G_{\text{passive}}(l+m, F) - M\Delta G_d, & m > M \end{cases}, \quad (5)$$

and

$$k'_0 \text{ active}(m) = \begin{cases} 0, & m < \delta \\ k_0 \exp[-a \min(M, \delta) \Delta G_d / k_B T], & \delta \leq m < \max(M, \delta) \\ k_0 \exp[-a(M + \delta - m) \Delta G_d / k_B T], & \max(M, \delta) \leq m < M + \delta \\ k_0, & M + \delta \leq m \end{cases}, \quad (6)$$

where a ($0 < a < 1$) is a dimensionless coefficient determined by the relative location of the activation barrier for helicase stepping motion within the step size. After taking into account the destabilization due to the helicase interaction with the fork in $\Delta G_{\text{active}}(l+m, F)$, the same method as shown in Equation 2 was used to calculate the probability $P_{\text{active}}(l, m, F)$ for DNA to open m bases in front of the helicase. Because of the additional energy term containing ΔG_d , the first M bases of dsDNA near the helicase have a greater probability of opening. As a result, the average helicase unwinding rate in the active mechanism, as calculated using Equation 1, is faster than that in the passive mechanism for a given step size.

There are four parameters in the active model: the step size δ , the interaction range M , the interaction potential increase per base ΔG_d , and the activation barrier coefficient a . The parameter a needs to be small to optimize the unwinding rate, but $a = 0$ is a physically unrealistic condition and singular limit (Betterton and Jülicher, 2005). To minimize the number of fit parameters, we set $a = 0.05$ (in fact, $a > 0.3$ would not fit our data). For each combination of δ and M , ΔG_d was tuned to produce the best fit of the model to the measured helicase unwinding force-velocity relation. There were different combinations of (δ , M) that produced reasonable fits, but all required that $M \geq \delta$. These results consist of a range of step sizes between 2–4 bp, interaction ranges ≥ 4 bp (depending on the step size), and interaction potential increases of 1–2 $k_B T$ per base (Figure S8). Figure 6B illustrates a good agreement between measured unwinding velocity dependence on force and simulated data with a step size of 2 bp, an interaction range of 6 bp, and interaction potential increase per base of 1.2 $k_B T$. The same set of parameters also correctly predicted the measured unwinding rate dependence

on DNA sequence (Figures 5A, S4, and S5). Therefore, these unwinding rate versus force and unwinding rate versus sequence results support an active unwinding model where the T7 helicase destabilizes a region of dsDNA near the junction and thus facilitates fork opening.

DISCUSSION

Degree of “Activeness” in DNA Unwinding by Helicase

This work provides a quantitative approach to determine if a helicase unwinds DNA passively or actively, and if actively, the degree of activeness (Figure 7D). The activeness may be quantitatively characterized by ΔG_d . The active model predicts that unwinding rate increases with ΔG_d and approaches the optimal unwinding rate (\sim ssDNA translocation rate) at $\sim 3.4 k_B T$ (the free energy to open a single GC base pair). For T7 helicase, the measured ΔG_d was ~ 1 –2 $k_B T$. Although our results support an active unwinding mechanism for T7 helicase, the model also indicates the helicase is not optimally active. It would be interesting to investigate where other helicases lie on the ΔG_d scale. The degree of activeness may also be characterized by the enhancement of unwinding rate from that of a passive unwinding mechanism. In our studies, over the range of forces examined, the measured unwinding rate was at least seven times higher than those predicted by the strictly passive unwinding model with the same step size.

Destabilization of the DNA Fork Junction by Helicases

Our results suggest that T7 helicase interacts with the fork junction and destabilizes a region of dsDNA near the junction to facilitate fork opening. This destabilization must ultimately be fueled by the free energy from the dTTP hydrolysis. The exact mechanism by which T7 helicase may destabilize the fork is not known. Structural and biochemical studies on T7 helicase have provided some intriguing clues. T7 helicase encloses one of the ssDNA within its central channel while excluding the other ssDNA at the junction (Hacker and Johnson, 1997; Ahnert and Patel, 1997). The helicase’s predominantly negatively charged exterior surface (Sawaya et al., 1999) should repel the negatively charged complementary strand of DNA, either in ssDNA or dsDNA forms. These interactions should occur when the helicase is within a few nm of the complementary DNA, given that the Debye-Huckel screening length is ~ 1 nm under physiological conditions (Israelachvili, 1992). This repulsion should weaken the base-pairing affinity of the dsDNA near the junction. If this repulsion is not sufficient to induce junction opening, the fork may begin to enter the central channel of the helicase as the helicase advances on the ssDNA. In this case, the complementary ssDNA will necessarily have to be severely bent near the channel entrance. The central channel of the helicase is only ~ 2 –3 nm in diameter (Sawaya et al., 1999; Singleton et al., 2000), which can comfortably accommodate ssDNA, may barely accommodate dsDNA of ~ 2 nm

diameter, and will not accommodate dsDNA together with the bent-back ssDNA. Considering ssDNA has a contour length of ~ 0.6 nm per nucleotide and a persistence length of ~ 0.8 nm (Smith et al., 1996; see also Figure S7), any significant bending of ssDNA over a couple of nucleotides will incur an energetic penalty, resulting in fork destabilization. It is conceivable that electrostatic repulsion together with ssDNA bending due to steric exclusion could expand the interaction between the helicase and the fork over a few bases near the junction. Therefore, by destabilization of the fork, the helicase may be able to “wedge” through the junction (Patel and Picha, 2000).

The physical mechanisms of fork junction destabilization for nonring-shaped helicases are still under investigation. Crystal structure (Velankar et al., 1999) and footprinting assays (Soultanas et al., 2000) of PcrA show that its 2B subdomain binds to dsDNA near the junction and distorts the double helix. Similarly the 2B subdomain of the structurally homologous UvrD also binds to the duplex DNA (Lee and Yang, 2006). For PcrA, mutations in the 2B domain abolished unwinding but retained the ssDNA translocation, suggesting an active unwinding mechanism (Soultanas et al., 2000). However, removal of the 2B subdomain from the structurally homologous Rep resulted in more efficient unwinding, suggesting that the 2B domain may instead be involved in inhibition of the unwinding activity (Cheng et al., 2002; Brendza et al., 2005). It has been suggested that RecBCD unwinds dsDNA with an active mechanism (Singleton and Wigley, 2002) based on its characteristic high translocation rate. The high rate is facilitated by two motor subunits, RecB and RecD, with each translocating on one of the two ssDNA toward the junction (Taylor and Smith, 2003; Dillingham et al., 2003). A third subunit, RecC, which is between the two motor subunits, contains a “pin” region (Singleton et al., 2004) where duplex DNA melting is believed to occur. Active destabilization may take place by the motor subunits pulling the junction against this pin region.

Strand Separation as a Major Barrier to Helicase Translocation

Many helicases, if not all, are capable of rapidly translocating along ssNA but dramatically slow down during unwinding (Kim et al., 2002; Jeong et al., 2004; Cheng et al., 2002; Brendza et al., 2005; Myong et al., 2005; Dillingham et al., 2000; Bertram et al., 2002; Fischer et al., 2004; Maluf et al., 2003). For these helicases, it appears that $\Delta G_d < \Delta G_{GC}$ (not optimally active, Figure 7D) so that strand separation at the junction represents a major obstacle to their forward translocation. Therefore, it is expected that the unwinding rate should also be dictated by the dsNA sequence at the fork, increasing at AT-rich regions and decreasing at GC-rich regions. As a corollary, the application of an external force to destabilize the fork should also facilitate unwinding. Indeed, T7 helicase follows such a prediction. T7 helicase is capable of translocating along ssDNA ~ 10 times faster than it can unwind dsDNA, as has been shown by this work and by previous studies (Kim et al., 2002; Jeong

et al., 2004; Stano et al., 2005). Our observation of unwinding rate dependence on dsDNA sequence and on force clearly indicates that strand separation is a major barrier for the T7 helicase. It is likely that all ring-shaped helicases share similar characteristics in both ssDNA translocation and dsDNA unwinding mechanisms.

Many non-ring-shaped helicases (Rep, PcrA, and UvrD) rapidly translocate along ssNA, and slow down when unwinding a dsNA fork (Cheng et al., 2002; Brendza et al., 2005; Myong et al., 2005; Dillingham et al., 2000; Bertram et al., 2002; Fischer et al., 2004; Maluf et al., 2003). This indicates that strand separation is a major barrier for nonring-shaped helicases as well. However, UvrD and HCV NS3 have been shown to have unwinding rates that are independent of the force destabilizing the fork (Dessinges et al., 2004; Dumont et al., 2006), consistent with unwinding not being limited by strand separation. This apparent contradiction for these nonring-shaped helicases, which is not observed in T7 helicase, may indicate some fundamental differences between the ring-shaped and nonring-shaped helicases in how the ssNA translocation is coupled to unwinding. When a nonring-shaped helicase encounters a junction, its translocation mechanism may be altered, not just slowed down as with T7 helicase. Indeed, monomers of UvrD and Rep are capable of translocating along ssDNA. However, unwinding seems to require the formation of a helicase dimer near the junction (Maluf et al., 2003; Fischer et al., 2004; Brendza et al., 2005; Myong et al., 2005).

T7 Helicase Interaction with DNA Polymerase

Helicase can unwind nucleic acids without accessory proteins but works more efficiently when coupled to them. Interestingly, the unwinding rate of T7 helicase is greatly enhanced and approaches that of ssDNA translocation in the presence of T7 DNA polymerase (Stano et al., 2005; Lee et al., 2006). This interdependence of helicase unwinding rate and DNA polymerase replication rate has been observed for homologous and heterologous helicases and polymerases (Delagoutte and von Hippel, 2001). The results from this study provide a simple explanation for these observations. This work suggests that the T7 helicase in the absence of the polymerase destabilizes the dsDNA near the fork junction by $\Delta G_d \sim 1\text{--}2 k_B T$ (per base), while ΔG_d needs to be $\sim 3.4 k_B T$ (GC base-pairing energy) in order to achieve the maximum unwinding rate (around the ssDNA translocation rate). In the current study, additional destabilization of the fork was provided by an application of a force to the junction. Similarly when T7 helicase is coupled with DNA polymerase, the polymerase may provide the additional destabilization energy of $\sim 2 k_B T$, equivalent to a destabilization force of ~ 14 pN, that is necessary to achieve a maximum rate.

EXPERIMENTAL PROCEDURES

Biological Materials

A 5.2 kilobase (kb) DNA construct with both a biotin label and a digoxigenin (dig) label was created as previously described (Koch et al.,

2002). Of this DNA, 4.1 kb was available for unwinding. The unwinding segment was derived from three repeats of the 5S rRNA sequence, each of which consists of five repeats of 207 bp (Figure S1). The three 5mers were joined together by 224 bp linking regions to form a construct with 17 pseudorepeats of ~200 bp. T7 helicase was prepared as described previously (Patel et al., 1992). The expressed protein was from gp4A', which consists of the helicase and primase.

Single-Molecule Sample Preparation

The sample preparation for the optical trapping experiments was similar to previously described (Koch et al., 2002) with the following modifications: Helicase was prepared by first incubating 2 μ M helicase monomer, 2mM dTTP, 3 mM EDTA, 0.02% Tween 20, and 50 mM NaCl in 20 mM Tris-HCl (pH 7.5) buffer at 22°C for 20 min. Helicase was then diluted to a final concentration of 2 nM monomer in 2 mM dTTP, 7 mM MgCl₂, 3 mM EDTA, 0.02% Tween 20, 50 mM NaCl, and 20 mM Tris-HCl (pH 7.5). DNA tethers were formed by first adding antidigoxigenin to the sample chamber, which binds nonspecifically to the coverglass surface. Next the digoxigenin end-labeled DNA construct was added to chamber, which was followed by the addition of streptavidin-coated 0.48 μ m polystyrene microspheres. Finally the helicase solution was flowed into the sample chamber just prior to data acquisition.

Single-Molecule Data Collection

Data were collected using a single beam optical trap as described previously (Koch et al., 2002). Experiments were conducted under constant force, position, or velocity as achieved via computer-controlled feedback. Data were low-pass filtered to 5 kHz and digitized at ~12 kHz, then were further averaged to 110 Hz. Experiments were conducted at a room temperature of 23.3°C. The temperature at the helicase was expected to have increased slightly to 25 \pm 1°C due to local heating by the trapping laser (Peterman et al., 2003). The acquired data signals were converted into force and number of base pairs unzipped as previously described (Koch et al. 2002), with the exception of using a more refined force-extension curve for ssDNA (Figure S7).

Data Analysis

For the sequence-dependent studies (Figure 5A), each measured force was aligned to a theoretical force for the initial 400 bp of mechanically unwound DNA, improving positional accuracy and precision to a few base pair (Shundrovsky et al., 2006). After alignment, an instantaneous unwinding rate at each sequence position was found by using a Gaussian weighted filter of 0.05 s (Adelman et al., 2002) and then re-sampling at 1 bp intervals along the sequence position. The final rate versus position curve was found by averaging over all of the traces at each position. For the unwinding rate versus force studies (Figure 6B), the rate was obtained by a line fit to each measured number of base pairs unwound versus time trace. Only data between the sequence positions of ~600 and ~807 bp (one pseudorepeat) were used for the fit. The final rate was obtained by averaging over all of the traces at each force.

Determination of Base-Pairing Energies

For simplicity ΔG_{bp} is assumed to only depend on if a base pair is AT (ΔG_{AT}) or GC (ΔG_{GC}). These energies were determined from unzipping DNA in the absence of helicase and then fitting the unzipping force results to a theoretical model (Bockelmann et al., 1997). This model was computed from a partition function using the free energies as a function of the number of base pairs unzipped and the end-to-end extension of the unzipped DNA: $\Delta G(n, x) = \sum_{i=1}^n \Delta G_{bp}(i) + 2n \int_0^{x/2n} F(x_{nt}) dx_{nt}$, where $F(x_{nt})$ is the force versus extension relation for one nucleotide of ssDNA (Figure S7). ΔG_{AT} and ΔG_{GC} were tuned to minimize the difference between the predicted and measured unzipping forces (Figure 5B), yielding best-fit values of 1.2 $k_B T$ and 3.4 $k_B T$, respectively.

For comparison, these values are comparable to, but ~10% smaller than, those estimated with DINAMelt (Markham and Zuker, 2005).

Simulation of Sequence-Dependent Unwinding Rate

To predict the sequence-dependent unwinding rate, Monte-Carlo simulations of helicase position versus time traces were generated using the active model with $\delta = 2$ nt, $M = 6$ bp, and $\Delta G_d = 1.2 k_B T$. An amount of noise comparable to that of experiments was added to the simulated traces, and the instantaneous unwinding rate at each base was obtained using the same data analysis method as was used for the measured single-molecule traces. The resulting predicted helicase-unwinding rate versus sequence-position (Figure 5A, green curve) is an average of 500 simulated traces.

Supplemental Data

Supplemental Data include eight figures, Discussion, and References and can be found with this article online at <http://www.cell.com/cgi/content/full/129/7/1299/DC1/>.

ACKNOWLEDGMENTS

We thank members of the Wang lab for helpful discussions and critical reading of the manuscript. We also thank R.C. Yeh, S. J. Koch, D.A. Wacker, and A. Shundrovsky for assistance during the initial stage of the project. We thank Y.J. Jeong and I. Donmez for providing purified T7 helicase protein. This research was supported by the Keck Foundation to M.D.W., GM55310 NIH grant to S.S.P., and a Molecular Biophysics Training Grant to Cornell.

Received: November 26, 2006

Revised: March 2, 2007

Accepted: April 24, 2007

Published: June 28, 2007

REFERENCES

- Adelman, K., La Porta, A., Santangelo, T.J., Lis, J.T., Roberts, J.W., and Wang, M.D. (2002). Single molecule analysis of RNA polymerase elongation reveals uniform kinetic behavior. *Proc. Natl. Acad. Sci. USA* 99, 13538–13543.
- Ahnert, P., and Patel, S.S. (1997). Asymmetric interactions of hexameric bacteriophage T7 DNA helicase with the 5'- and 3'- tails of forked DNA substrate. *J. Biol. Chem.* 272, 32267–32273.
- Amaratunga, M., and Lohman, T.M. (1993). *Escherichia coli* rep helicase unwinds DNA by an active mechanism. *Biochemistry* 27, 6815–6820.
- Bertram, R.D., Hayes, C.J., and Soutanas, P. (2002). Vinylphosphate internucleotide linkages inhibit the activity of PcrA DNA helicase. *Biochemistry* 41, 7725–7731.
- Betterton, M.D., and Jülicher, F. (2003). A motor that makes its own track: helicase unwinding of DNA. *Phys. Rev. Lett.* 91, 258103.
- Betterton, M.D., and Jülicher, F. (2005). Opening of nucleic-acid double strands by helicases: active versus passive opening. *Phys. Rev. E. Stat. Nonlin. Soft Matter Phys.* 71, 011904.
- Bockelmann, U., Essevez-Roulet, B., and Helset, F. (1997). Molecular stick-slip motion revealed by opening DNA with piconewton forces. *Phys. Rev. Lett.* 79, 4489–4492.
- Brendza, K.M., Cheng, W., Fischer, C.J., Chesnik, M.A., Niedziela-Majka, A., and Lohman, T.M. (2005). Autoinhibition of *Escherichia coli* Rep monomer helicase activity by its 2B subdomain. *Proc. Natl. Acad. Sci. USA* 102, 10076–10081.
- Chen, Y.Z., Zhuang, W., and Prohofskey, E.W. (1992). Energy flow considerations and thermal fluctuational opening of DNA base pairs at a replicating fork: unwinding consistent with observed replication rates. *J. Biomol. Struct. Dyn.* 10, 415–427.

- Cheng, W., Brendza, K.M., Gauss, G.H., Korolev, S., Waksman, G., and Lohman, T.M. (2002). The 2B domain of the *Escherichia coli* Rep protein is not required for DNA helicase activity. *Proc. Natl. Acad. Sci. USA* *99*, 16006–16011.
- Delagoutte, E., and von Hippel, P.H. (2001). Molecular mechanisms of the functional coupling of the helicase (gp41) and polymerase (gp43) of bacteriophage T4 within the DNA replication fork. *Biochemistry* *40*, 4459–4477.
- Delagoutte, E., and von Hippel, P.H. (2002). Helicase mechanisms and the coupling of helicases within macromolecular machines part I: structures and properties of isolated helicases. *Q. Rev. Biophys.* *35*, 431–478.
- Dessinges, M.N., Lionnet, T., Xi, X.G., Bensimon, D., and Croquette, V. (2004). Single-molecule assay reveals strand switching and enhanced processivity of UvrD. *Proc. Natl. Acad. Sci. USA* *101*, 6439–6444.
- Dillingham, M.S., Wigley, D.B., and Webb, M.R. (2000). Demonstration of unidirectional single-stranded DNA translocation by PcrA helicase: measurement of step size and translocation speed. *Biochemistry* *39*, 205–212.
- Dillingham, M.S., Spies, M., and Kowalczykowski, S.C. (2003). RecBCD is a bipolar DNA helicase. *Nature* *423*, 893–897.
- Dohoney, K.M., and Gelles, J. (2001). γ -sequence recognition and DNA translocation by single RecBCD helicase/nuclease molecules. *Nature* *409*, 370–374.
- Dumont, S., Cheng, W., Serebrov, V., Beran, R.K., Tinoco, I., Jr., Pyle, A.M., and Bustamante, C. (2006). RNA translocation and unwinding mechanism of HCV NS3 helicase and its coordination by ATP. *Nature* *439*, 105–108.
- Egelman, E.H., Yu, X., Wild, R., Hingorani, M.M., and Patel, S.S. (1995). Bacteriophage T7 helicase/primase proteins form rings around single-stranded DNA that suggests a general structure for hexameric helicases. *Proc. Natl. Acad. Sci. USA* *92*, 3869–3873.
- Enemark, E.J., and Joshua-Tor, L. (2006). Mechanism of DNA translocation in a replicative hexameric helicase. *Nature* *442*, 270–275.
- Fischer, C.J., Maluf, N.K., and Lohman, T.M. (2004). Mechanism of ATP-dependent translocation of *E. coli* UvrD monomers along single-stranded DNA. *J. Mol. Biol.* *344*, 1287–1309.
- Geiselmann, J., Wang, Y., Seifried, S.E., and von Hippel, P.H. (1993). A physical model from the translocation and helicase activities of *Escherichia coli* transcription termination protein Rho. *Proc. Natl. Acad. Sci. USA* *90*, 7754–7758.
- Hacker, K.J., and Johnson, K.A. (1997). A hexameric helicase encircles one DNA strand and excludes the other during DNA unwinding. *Biochemistry* *36*, 14080–14087.
- Israelachvili, J.N. (1992). *Intermolecular and Surface Forces*, Second Edition (San Diego: Academic Press).
- Jeong, Y.J., Levin, M.K., and Patel, S.S. (2004). The DNA-unwinding mechanism of the ring helicase of bacteriophage T7. *Proc. Natl. Acad. Sci. USA* *101*, 7264–7269.
- Johnson, D.S., Patel, S.S., and Wang, M.D. (2004). Single molecule study of the molecular motor T7 helicase using optical tweezers. 2004 Biophysical Society Meeting Abstracts. 1703-Pos. *Biophys. J. (Supplement 86)*, 328A.
- Kaplan, D.L., and O'Donnell, M. (2004). Twin DNA pumps of a hexameric helicase provide power to simultaneously melt two duplexes. *Mol. Cell* *15*, 453–465.
- Kim, D.E., Narayan, M., and Patel, S.S. (2002). T7 DNA helicase: a molecular motor that processively and unidirectionally translocates along single-stranded DNA. *J. Mol. Biol.* *321*, 807–819.
- Kim, J.L., Morgenstern, K.A., Griffith, J.P., Dwyer, M.D., Thomson, J.A., Murcko, M.A., Lin, C., and Caron, P.R. (1998). Hepatitis C virus NS3 RNA helicase domain with a bound oligonucleotide: the crystal structure provides insights into the mode of unwinding. *Structure* *6*, 89–100.
- Koch, S.J., Shundrovsky, A., Jantzen, B.C., and Wang, M.D. (2002). Probing protein-DNA interactions by unzipping a single DNA double helix. *Biophys. J.* *83*, 1098–1105.
- Lee, J.B., Hite, R.K., Hamdan, S.M., Xie, X.S., Richardson, C.C., and van Oijen, A.M. (2006). DNA primase acts as a molecular brake in DNA replication. *Nature* *439*, 621–624.
- Lee, J.Y., and Yang, W. (2006). UvrD helicase unwinds DNA one base pair at a time by a two-part power stroke. *Cell* *127*, 1349–1360.
- Lohman, T.M., and Bjornson, K.P. (1996). Mechanisms of helicase-catalyzed DNA unwinding. *Annu. Rev. Biochem.* *65*, 169–214.
- Maluf, N.K., Fischer, C.J., and Lohman, T.M. (2003). A dimer of *Escherichia coli* UvrD is the active form of the helicase *in vitro*. *J. Mol. Biol.* *325*, 913–935.
- Markham, N.R., and Zuker, M. (2005). DINAMelt web server for nucleic acid melting prediction. *Nucleic Acids Res.* *33*, W577–W581.
- Matson, S.W., and Richardson, C.C. (1983). DNA-dependent nucleoside 5'-triphosphatase activity of the gene 4 protein of bacteriophage T7. *J. Biol. Chem.* *258*, 14009–14016.
- Matson, S.W., Tabor, S., and Richardson, C.C. (1983). The gene 4 protein of bacteriophage T7. Characterization of helicase activity. *J. Biol. Chem.* *258*, 14017–14024.
- Myong, S., Rasnik, I., Joo, C., Lohman, T.M., and Ha, T. (2005). Repetitive shuttling of a motor protein on DNA. *Nature* *437*, 1321–1325.
- Patel, S.S., and Hingorani, M.M. (1993). Oligomeric structure of bacteriophage T7 DNA primase/helicase proteins. *J. Biol. Chem.* *268*, 10668–10675.
- Patel, S.S., and Picha, K.M. (2000). Structure and function of hexameric helicases. *Annu. Rev. Biochem.* *69*, 651–697.
- Patel, S.S., Rosenberg, A.H., Strudier, F.W., and Johnson, K.A. (1992). Large scale purification and biochemical characterization of T7 primase/helicase proteins. Evidence for homodimer and heterodimer formation. *J. Biol. Chem.* *267*, 15013–15021.
- Perkins, T.T., Li, H.W., Dalal, R.V., Gelles, J., and Block, S.M. (2004). Forward and reverse motion of single RecBCD molecules on DNA. *Biophys. J.* *86*, 1640–1648.
- Peterman, E.J.G., Gittes, F., and Schmidt, C.F. (2003). Laser-induced heating in optical traps. *Biophys. J.* *84*, 1308–1316.
- Richardson, C.C. (1983). Bacteriophage T7: minimal requirements for the replication of a duplex DNA molecule. *Cell* *33*, 315–317.
- Sawaya, M.R., Guo, S., Tabor, S., Richardson, C.C., and Ellenberger, T. (1999). Crystal structure of the helicase domain from the replicative helicase-primase of bacteriophage T7. *Cell* *99*, 167–177.
- Shundrovsky, A., Smith, C.L., Lis, J.T., Peterson, C.L., and Wang, M.D. (2006). Probing SWI/SNF remodeling of the nucleosome by unzipping single DNA molecules. *Nat. Struct. Mol. Biol.* *13*, 549–554.
- Singleton, M.R., and Wigley, D.B. (2002). Modularity and specialization in superfamily 1 and 2 helicases. *J. Bacteriol.* *184*, 1819–1826.
- Singleton, M.R., Sawaya, M.R., Ellenberger, T., and Wigley, D.B. (2000). Crystal structure of T7 gene 4 ring helicase indicates a mechanism for sequential hydrolysis of nucleotides. *Cell* *101*, 589–600.
- Singleton, M.R., Dillingham, M.S., Gaudier, M., Kowalczykowski, S.C., and Wigley, D.B. (2004). Crystal structure of RecBCD enzyme reveals a machine for processing DNA breaks. *Nature* *432*, 187–193.
- Smith, S.B., Cui, Y., and Bustamante, C. (1996). Overstretching B-DNA: the elastic response of individual double-stranded and single-stranded DNA molecules. *Science* *271*, 795–799.
- Soultanas, P., Dillingham, M.S., Wiley, P., Webb, M.R., and Wigley, D.B. (2000). Uncoupling DNA translocation and helicase activity in PcrA: direct evidence for an active mechanism. *EMBO J.* *19*, 3799–3810.

Soultanas, P., and Wigley, D.B. (2001). Unwinding the 'Gordian knot' of helicase action. *Trends Biochem. Sci.* 26, 47–54.

Spies, M., Bianco, P.R., Dillingham, M.S., Handa, N., Baskin, R.J., and Kowalczykowski, S.C. (2003). A molecular throttle, the recombination hotspot χ controls DNA translocation by the RecBCD helicase. *Cell* 114, 647–654.

Stano, N.M., Jeong, Y.J., Donmez, I., Tummalapalli, P., Levin, M.K., and Patel, S.S. (2005). DNA synthesis provides the driving force to accelerate DNA unwinding by a helicase. *Nature* 435, 370–373.

Tabor, S., and Richardson, C.C. (1981). Template recognition sequence for RNA primer synthesis by gene 4 protein of bacteriophage T7. *Proc. Natl. Acad. Sci. USA* 78, 205–209.

Taylor, A.F., and Smith, G.R. (2003). RecBCD enzyme is a DNA helicase with fast and slow motors of opposite polarity. *Nature* 423, 889–893.

Velankar, S.S., Soultanas, P., Dillingham, M.S., Subramanya, H.S., and Wigley, D.B. (1999). Crystal structures of complexes of PcrA DNA helicases with a DNA substrate indicate an inchworm mechanism. *Cell* 97, 75–84.

von Hippel, P.H., and Delagoutte, E. (2001). A general model for nucleic acid helicases and their "coupling" within macromolecular machines. *Cell* 104, 177–190.

Wong, I., and Lohman, T.M. (1992). Allosteric effects of nucleotide cofactors on *Escherichia coli* Rep helicase-DNA binding. *Science* 256, 350–355.